Determining the Effects of Galectin/GM1 Interaction on Cellular Membrane Structure and Organization

by

D. Browne, Y. Weissbarth, H. J. Gabius, J. Majewski, C. Vander Zanden

B.S. Biochemisty, University of Colorado, 2020

A Portfolio submitted to the Honors Program Faculty of the

University of Colorado at Colorado Springs

in partial fulfillment of the

requirements for the UCCS Honors Program

2020

Student explicitly grants the copyright permission to UCCS Honors Program to post this portfolio report on the UCCS Honors Program Website, other selected UCCS platforms, including UCCS Communique, and at the UCCS Honors Program Symposium Proceedings website.

Danielle Browne	*August 3, 2020*
Signed by the Student	Date

This portfolio for the UCCS Honors Program
by

Name of the student

has been approved by the

UCCS Honors Program

by

Dr. Crystal Vander Zanden

Research Mentor Name

Dr. Sudhanshu Semwal

Reader One: Honors Program Faculty

Robert E. Sackett

Reader Two: Honors Program Faculty

Browne, Danielle (UCCS Honors Program: ML or UH)

August 3, 2020

Date

Honors Program Portfolio mentored by Dr. Crystal Vander Zanden

Abstract

Lectin and glycolipid interactions are of emerging interest in biochemistry. These interactions take part in a vast array of cellular functions such as signaling, regulation, and adhesion which could serve as potential therapeutic tools for a variety of immune, inflammatory, and neurodegenerative diseases. Lectin and glycolipid interactions however are extremely complex and multidimensional, creating a challenge to isolate specific chains of cause and effect which are necessary to understand for potential medical use. As a part of the Vander Zanden research lab at UCCS, we have performed experiments to help elucidate the effects of wild type Gal-1, Gal-3NT/1, and the mutants Gal-1 [8S] Gal-1 to determine their interactions with glycolipid GM1. The goal was to investigate if the mutants with extended repeat domains produce different results than the wild type protein, with implications for improving our understanding of cellular functions. Experiments using Langmuir trough techniques, x-ray reflectivity (XR), and grazing incidence x-ray diffraction (GIXD) have allowed the elucidation of membrane structure and organization after the introduction of the galectin variants. Each of these experiments were done using a ratio of 80:20 DPPC lipid and ganglioside GM1 within the model membrane studied. These experiments combined with understanding of the sugar code presented along the surface of cellular membranes can help begin to unveil the function of the interactions between GM1 and Gal-1. However, there is much extensive future work *still* to be done before this research is able to be completed in a clinical setting due to the complexity of these signaling interactions, bringing our research to fruition. The complexity of interactions is the focus of the proposed research to understand cellular communication.

TABLE OF CONTENTS

TABLES

FIGURES

Introduction

Galectins

Lectins are glycan-binding proteins secreted from the Golgi apparatus and endoplasmic reticulum that exist on the extracellular surface of membranes and recognize glycoconjugates on neighboring cells.[1] A specific class of lectins, galectins, have a conserved β-galactoside binding site within their carbohydrate recognition domains (CRD) (Fig. 1).[2]

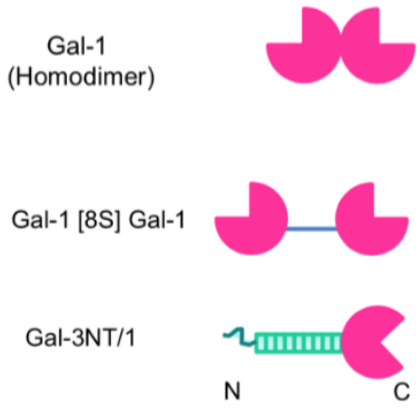

Figure 1. Structural domains of WT Gal-1 and mutants studied.

Galectin-1 (Gal-1) is a homodimeric protein with two identical CRDs exhibiting β jelly-roll topology. The β jelly-roll is a protein folding pattering where amino acids are organized in antiparallel β-sheets which then roll themselves into their final conformation.[2] The two CRDs associate through hydrophobic interactions, allowing them to crosslink binding partners on the membrane surface.[2] They promote cell vital activity such as cell-cell and cell-inter-cellular matrix adhesion as well as transmission of intercellular signals.[2] They can also be used as

markers of cellular transformation or mediators of inflammation.[2] The concentration of galectins within the cell is *theorized* to be mediated by some stress responses such as inflammation and malignancy.[2] These signals prompt the destruction of vesicles storing galectins so that they may release and interact with carbohydrate domains on the membrane surface.[2]Once lectins are able to reach the cell surface, they are able to perform their function as signaling molecules. One of the most notable examples of this signaling process is the interaction of galectins with activated T-cells to induce apoptosis.[3] Gal-1 specifically has been shown to have protective effects against autoimmune encephalitis in mice.[3] This disease is a paralytic T-cell mediated disease caused by immune dysregulation.[3] Gal-1 is able to induce apoptosis in the unregulated activated T-cells to prevent them destroying myelin basic proteins in neurons.[3] Similarly, inflammatory diseases such as hepatitis, T-cell dependent liver disease, and rheumatoid arthritis are all caused by immune dysregulation, implicating Gal-1 as a potential **therapeutic** tool.[3]

Though Gal-1 has been also shown to be therapeutically beneficial in some cases of inflammatory disease and carcinoma cells, it can have the opposite effect, favoring tumor growth in glioblastoma and pancreatic cancer cells by inducing different signaling pathways.[4] Gal-1 is also an effective diagnostic marker in thyroid cancer progression.[5] The galectin is completely absent in all benign thyroid tumor lesions but is highly expressed on the surface of malignant thyroid cancer cells, most likely due to its function as a growth promoter.[5] Experiments in mice showed that the deletion of Gal-1 enhances the

longevity of the mice while also reducing the proliferation and invasiveness of malignant cells.[5] Gal-1 has also been found to enhance flu virus binding to cell hosts by restoring the ability for the virus to infect cells without adequate influenza docking points.[6] Influenza has surface proteins presenting complex oligosaccharide chains that bind with Gal-1 to gain entry into the cell. Upon exiting the host membrane, the virus disconnects the galectins from their docking sites and carries them to the next host cell for easier infiltration.[6] Similar mechanisms for infection through galectins occur with human immunodeficiency virus (HIV) because the galectins function as adhesion proteins.[6] These differing functions make Gal-1 a very versatile immune regulator, but caution must be exercised when using it therapeutically to prevent adverse effects which are currently not understood.

Glycolipids

Glycolipids are lipids that are covalently bound to sugar molecules at their head group and protrude from the cell membrane. Gangliosides are glycolipids covalently bound to complex oligosaccharides containing a sialic group.[7] GM1, a ganglioside, is a key component for neuronal signaling and regulation. It's interactions drive microdomain regulation, neuronal differentiation, immune cell reactivity, and neural cell development and viability.[8] The glycan units on the head of the lipid protrude from the membrane and promote selective interactions with other glycoconjugates or proteins.[8] The ceramide tail is also important to the function of GM1 as it allows the molecule to be firmly anchored within the membrane due to hydrophobic interactions. The lipid tail packing structure allows

the hydrophilic oligosaccharide head to be readily accessible to reactive partners.[8] Gangliosides are predominately found in lipid rafts which can be defined as dense, ordered regions of the bilayer that often contain glycolipids and membrane proteins.[8] These raft domains act as points of signaling, adhesion, and mediation of cell-cell interactions.[8] In order to regulate the concentration of GM1 present in the membrane, derivatives such as GDIa can be modified with sialidase enzymes to remove extra sialic groups and transform the derivatives into GM1.[8] GM1 plays a role in formation and stabilization of the raft microdomain, however upon interaction with neurotoxic proteins such as β-amyloid, they can be extracted from the membrane which quickly degrades the integrity of the neuron.[8] This phenomena occurs in individuals with Parkinson's and Alzheimer's disease.[8] LIGA20 (a synthetic GM1 that can cross the blood brain barrier) has benefited these patients in preclinical trials likely due to the functional restoration of the lost GM1.[8] GM1 also modulates calcium ion influx across the membrane.[8] The elevation of GM1 alongside Ca^{2+} influx promotes regeneration of damaged peripheral nerves in the PNS system.[8] These elevated levels begin a cell signaling pathway that induces axonal growth. Crosslinking of GM1 by proteins also induces calcium influx which promotes axon growth in both the PNS and CNS.[8] However, there is a downside to the restorative properties of GM1 as it also takes part in inducing outgrowth of neuroblastoma cells.[8] Similar to the double-edged nature of Gal-1, including GM1 in therapeutic approaches requires extensive knowledge of the systems they can affect. Both of these molecular actions are dependent on concentration, cell-type, and environment,

making it extremely difficult to pinpoint where the altered use of them would benefit and harm a potential patient.

The Sugar Code

Gal-1 and GM1 are not the only molecules capable of such a wide array of cellular modulation. They are both components of a largely unexplored cellular communication system called the glycocode, or more commonly the sugar code. The use of specific saccharides at the cell surface by glycolipids and glycoproteins to convey information is an extremely complex and variable process that stems from post translational modifications of lipids (Fig.4).[1] This code presented at the cell surface is then read by lectins to signal cellular changes. The sequence and shape of the oligosaccharides presented underlie the specificity for lectin binding, acting as chemoattractants.[4] Many enzymes are involved in the process for creating a mass variety of saccharide head groups which allows for incredible intricacy and versatility for the signaling system.[4] In essence, these enzymes are spelling out instructions for the lectins to read with each sugar acting as a letter, and each oligosaccharide a word for the lectin to translate into action. The enzymes are responsible for reprograming the sugar code to respond to stress signals like malignancy which allow lectins to signal for action such as inducing apoptosis (programmed cell death) in tumor cells.[4] These oligosaccharide groups can also affect protein-protein interactions by changing the conformation of the bound protein so that it may interact with another protein.[4] The lectin binding of these sugar groups is very intricate and specific with some lectins having up to 14 different folds with the capacity for glycan

binding.[4] These vast amounts of potential binding sites allows lectins to be multivalent and bind to more than one sugar group at a time, further increasing the sophistication of the sugar code.[7] The lectins are able to detect whether hydroxyl groups are in axial or equatorial position, the charge of the group, as well as the conformation and orientation.[4] This complexity allows for a vast amount of information to be stored in a small area with optimal responsiveness. The homodimeric binding domains of Gal-1 are able to crosslink oligosaccharide presenting molecules in order to communicate information from two different sites.[4] Gal-1 crosslinking with GM1 induces immunosuppression upon an inflammatory stress signal.[9] The activation of T-cells up-regulates Gal-1 upon crosslinking, mediating calcium flux in order to activate downstream immunosurpession.[9] When autoreactive T-cells escape thymic deletion, their overactivity can cause a variety of autoimmune disorders such as type I diabetes, rheumatoid arthritis, and multiple sclerosis.[9] These negative outcomes are why the Gal-1/GM1 interaction is essential to preventing hyperinflammation that could be damaging to the body. Studies in mice with autoimmune disorders have shown that the supplementation of Gal-1 and CtxB (another GM1 counterreceptor) decreases the severity of the disease presented. As a part of the sugar code, Gal-1/GM1 interactions have a diverse array of implications, some of which could be key therapeutic targets of the future.

Grazing Incidence X-Ray Diffraction and Langmuir Monolayers

Due to the complex nature of the glycocode and associated reactions, it can be difficult to study with typical laboratory experiments. Many researchers

make use of X-ray beams' ability to be diffracted and reflected from a model cell membrane to elucidate structural aspects of the interaction being studied. In order to prepare a model membrane, there are several techniques that can be used to produce a variety of models such as vesicles and bilayers. The model used for these 2D x-ray scattering experiments is the lipid monolayer created with a Langmuir trough. The trough is a shallow dish in which lipids can be spread across the air/water interface to a certain surface pressure where they then organize into a monolayer film with the hydrophilic heads submerged in water and the hydrophobic tails protruding from the air/water interface. A platinum plate called the Wilhelmy plate is able to detect the surface pressure and Langmuir trough software is able to calculate the average molecular area of the monolayer throughout the experiment. The measured surface pressure and average molecular area is used indicate the insertion of a protein or other lipophilic structure into the monolayer. When insertion events occur, the lipids are pushed aside to make room for the new molecule entering the interface and this 'pushing' causes an increase in surface pressure detected by the Wilhelmy balance. Either the trough area or surface pressure can be held constant with barriers in order to isolate one variable and observe how molecular interactions change that variable only, giving a clearer picture of activity. Once the monolayer is established GIXD allows for the detection of in-plane membrane structure.[10] X-rays permit radiation to weakly couple with scattering objects which then diffract the radiation, allowing for structural determination of crystalline arrangements.[11] In order for this phenomenon to occur, the x-ray beam is set to a glancing angle

(α) which is smaller than the critical angle (α_c) for a total external reflection.[10] Upon contact with the model membrane, the plane wave within the material factorizes and propagates within the plane of the monolayer surface.[10] The intensity, which varies with the glancing angle, is measured by squaring the amplitude just below the surface.[10] The evanescent wave amplitude (T(α)) is a result of the interference from the incident wave and reflected wave. When regions of the monolayer are ordered (lipid condensed phase) versus disordered (lipid expanded phase) the evanescent wave is Bragg scattered and diffractions are observed from lattice planes (h,k), and their distance (d_{hk}) at an angle (θ_{hk}) agrees with the Bragg condition (Eq. 1).[10]

$$\lambda = 2d_{hk}\sin\theta_{hk} \quad (1)$$

Equation 1. Bragg's condition used to determine the 2D structure of the monolayer surface.[10]

The vertical angle is determined by a position sensitive detector which can delineate the lateral (q_{xy}) and vertical (q_z) components of the scattering vector.[10] The diffraction signal is the result of the average structure of all material within the footprint of the beam.[12] Each of these measurements done using GIXD are extremely relevant when attempting to define the in-plane packing structure of ordered membrane domains as well as their vertical tilt and direction. This data can then be plugged into equations to determine the topological organization of the condensed domains. The coherence length (L_c) is determined by (L_c=(0.9)(2π)/FWHM) to describe the length of the coherently scattered object.

Lattice spacing (d) is determined by ($d=2\pi/q_{xy}$) to describe the space between molecules. These calculations in addition to the parameters measured all contribute to the description of the unit cell. In this experiment, the GIXD data is consistent with an oblique unit cell. Experimentally, this is useful when determining if protein interactions disturb the crystalline packing. Comparing the profiles of a membrane, and membrane with added protein allows researchers to describe the manner of protein insertion into the membrane and how it may reorganize, increase, or decrease the presences of lipid condensed domains.

Specular X-Ray Reflectivity

Now that we have addressed the horizontal planar structure of a monolayer with GIXD, we will need to use specular x-ray reflectivity (XR) to gain information about the vertical structure of the membrane. A simple way to grasp this method is to consider the phenomena of oil on the surface of a puddle which is commonly seen day to day. The colors that are seen are caused by interference of light reflected from the oil-air interface and the oil-water interface.[10] This concept is mirrored when using XR where the incident beam is at a fixed wavelength or “color” when it is approaching the sample and when it is reflected.[10] This monochromatic beam is then deflected towards the monolayer at angle α_i. A horizontal slit of height (h) placed in front of the trough limits the beam footprint to be h/α.[10] The beam intensity is registered by a detector behind the slit, meanwhile the slit and trough height track the beam with elevators.[10] Using the assumption that intensity of water is an infinitely sharp peak, Snell and Fresnel’s laws can be used to describe the intensity of monolayer components.[10]

Often, the chamber containing the trough is flushed with helium in order to reduce intensity disruption by vapors and the need to account for these vapors interference. We begin using Snell and Fresnel's law by considering the three plane waves of refraction and reflection (I, R, or T) (Eq. 2 and 3).[10]

$$\psi_j = \alpha_j e^{ikj\cdot r},\ j = I, R\ or\ T \quad (2)$$

$$k = |k_I| = |k_R| = |k_T|/n \quad (3)$$

The wavenumber k is related to the wavelength λ(wavelength) by k=2π/λ and the coefficient α_j is related by the fact that ψ (plane waves) must be continuous across the interface.[10] These geometrical relations lead to Fresnel's Law and Fresnel reflectivity (Eq. 4,5, and 6).[10]

$$\left(1 + \frac{\alpha_R}{\alpha_I}\right)\alpha' = \left(1 - \frac{\alpha_R}{\alpha_I}\right)\alpha \quad (4)$$

$$R \equiv \frac{\alpha_R}{\alpha_I} = \frac{\alpha - \alpha'}{\alpha + \alpha'} \quad (5)$$

$$R_F = \left|\frac{\alpha - \alpha'}{\alpha + \alpha'}\right|^2 \quad (6)$$

Roughness is also measured using Fresnel's Law which describes the thermally excited capillary waves on the surface.[12] After conducting the experiment, the measured reflectivity can be divided by the Fresnel reflectivity and inverted to produce the lateral electron density in the z direction as well as thickness (the

length of the different regions of electron density).[12] The electron density profile allows us to see the different slabs of electron density within the monolayer, and when fit with a slab model, delineates the spacing and position of different membrane components: lipid head, lipid tails, glycans, proteins, etc. A fitting program (Igor pro used in this experiment) measures the models' deviation from the observed data using assumed average density and the width of the air-film interface.[12] The algorithm then enters them as weighted terms into χ^2 which is minimized by the fitting algorithm in order to minimize error.[12] Using in combination, GIXD and XR, an accurate description of the organization of the monolayer in the x,y, and z directions can be obtained to elucidate the structural changes that occur upon protein interaction with the model membrane.

Materials and Methods

Materials

The proteins, Gal-1, Gal-3NT/1, and Gal-1 [8S] Gal-1 were prepared by recombinant expression and purified by the lab of Dr. Hans-Joachim Gabius. The purified protein samples were lyophilized and stored at -80°C to prevent denaturation and reconstituted in pure water to a concentration of 1mg/mL. From this stock the protein was aliquoted in single use quantities then stored again at -80°C. Phosphate buffer and sodium chloride were present in solution after reconstitution due to salts present in the lyophilized protein. TexasRed-DHPE was used in fluorescence microscopy experiments (data not included) and purchased from Thermo Fischer Scientific (Waltham, WA). 1,2-dipalmitoyl-sn-glycero-3-phosphocholine (DPPC) and Galectin GM1 were purchased from

Avanti Polar Lipids (Alabaster, AL) and used without further purification. Stock solutions were made in acid washed glass vials using an 80:20 or 95:5 mol% ratio of DPPC:GM1 and an 80:20 ratio (v/v) of chloroform and methanol as a solvent. TexasRed-DHPE was added to these stocks if fluorescence microscopy was being used in a 0.5 mol% ratio. The organic solvents were purchased from Thermo Fischer Scientific (Waltham, WA). The stock lipid solution was diluted from 3.33mg/mL to 0.2mg/mL to be used in experiments and stored at -20°C.

Lipid Monolayer Insertion Assays

Langmuir trough experiments were conducted in a 40mL Teflon Langmuir trough with movable Delrin barriers that could be held at a constant average molecular area of surface pressure. The Langmuir trough is a KSV NIMA small Langmuir trough for microscopy by Nanoscience Instruments (Phoenix, AZ). The experiments were conducted using a pure water subphase held constant at 25°C while the surface pressure of the interface was being monitored by a Wilhelmy plate balance. 45uL of the 0.2mg/mL lipid solution containing 94.5:5:0.5 mol% of DPPC:GM1:TexasRed-DHPE was deposited on the water surface using a Hamilton syringe to add the solution in small increments over the whole surface. After the lipids were deposited, 10 minutes were allowed to evaporate the chloroform/methanol solvent. The lipids were then compressed to the target surface pressure of 16mN/m and held at that pressure for 15 minutes to ensure the stability of the monolayer. The surface pressure was held constant using the moveable barriers in a feedback loop to adjust the monolayer area in response to surface pressure fluctuations. After stabilization of the monolayer, 500uL of

1mg/mL protein was injected underneath the monolayer to a concentration of 0.0125mg/mL in the trough. The barriers were fixed at a constant area so any effects of the protein insertion could be seen as an increase of surface pressure.

X-Ray Scattering

The GIXD and XR experiments were performed using synchrotron x-rays at the Advanced Photon Source at Argonne National Laboratories (Sector 15 NSF's ChemMatCars). A 20mL Teflon Langmuir trough was filled with degassed water subphase and held at room temperature (23.0 +/- 0.5 °C). The lipid solution was deposited to the air/water interface as they were in above experiments but using a 0.2mg/mL solution of 80:20 mol% DPPC:GM1 (this ratio provided a higher GM1 concentration to increase detection) dissolved in 8:2 chloroform:methanol. The lipids were deposited to the target surface pressure of 20mN/m. The monolayer was allowed to stabilize, and data was collected to use for comparison against the membrane with protein. In order to limit oxidative damage and vapor disruption to the sample during radiation, the trough was sealed in a canister and flushed with helium until the gaseous oxygen content was below 2%. The x-ray wavelength was 1.24 Angstroms and the x-rays were detected with a Dectris PILATUS 100k detector. The trough was moved 1mm after each scan to account for sample damage due to x-ray exposure, allowing each scan to take place on a new undamaged sample. XR data was collected 2 hours and 5 hours post injection (2 hours was not long enough to produce significant evidence of protein insertion) and GIXD data was collected 3 hours post injection.

Data Analysis

StochFit was used to perform model-independent fitting of the XR data that was used as a reference for more precise model-dependent fits. The Motofit data analysis packing in Igor Pro was used for model-dependent fitting of the XR data. By entering the reported values of thickness, SLD, and roughness obtained from StochFit, they were used as a starting point for the model-dependent curve fitting. By changing variable boundaries and using a genetic fit model, the fit was optimized with χ^2 values below 5 and parameter errors below or as close as possible to 10%. The MultiPeak Fit 2.0 package in Igor Pro was used to fit the GIXD data. The software fit the drawn peaks to the data using Lorentzian peaks and a cubic baseline with the fit weighting adjusted based on measured errors for each data point. The fits all had errors less than 10% for the full width half max (FWHM), peak area, and peak location. The x-ray reflectivity and diffraction images were integrated using Python software built by beamline support scientists (https://chemmatcars.uchicago.edu/software/).

Results

Langmuir Trough Experiments

The surface area was recorded over the duration of the experiment (6 hours) while the barriers were fixed at a constant trough area. The monolayer (89.5:20:0.5 mol% DPPC:GM1:TexasRed DHPE) was stabilized at a pressure of 16mN/m and a temperature of 25 °C. After stabilization, protein was inserted (WT

Gal-1, Gal-3NT/1, and Gal-1 [8S] Gal-1 used in separate experiments).The data shows clear evidence of protein insertion for each protein tested under the same conditions (Fig. 2). Each protein produces a surface pressure increase during the time of insertion until a plateau is reach upon which the maximum amount of protein has inserted into the monolayer. The relative rate of insertion can be seen in the slope of the three traces, with the steeper slopes indicating a faster insertion.

GIXD

The GIXD diffraction peaks are shown in Figure 3, where there is no evidence of structural reorganization of the lipid condensed domains measured. For each protein measured as well as the membrane, there were consistently two peaks at q_{xy} positions of ~1.39 and 1.47 $Å^{-1}$, with the later having a higher intensity and sharper peak than the former and both were fit using Lorentzian peaks. The data presented was obtained at a time of 3 hours post injection. Upon protein interaction there is a decrease in intensity and integrated peak area especially prominent in the Gal-1 [8S] Gal-1 scan (Table 1). The condensed domains of the monolayer consist of a 2D crystalline structure with calculated coherence length in the x-y plane. The similar diffraction peaks observed for all four experiments indicates that the protein interactions do not in fact reorganize the pattern of the lipid condensed domains. However, each protein decreased the integrated peak area and intensity, indicating that the proteins interact with lipids in the ordered phase and cause partial packing disruption.

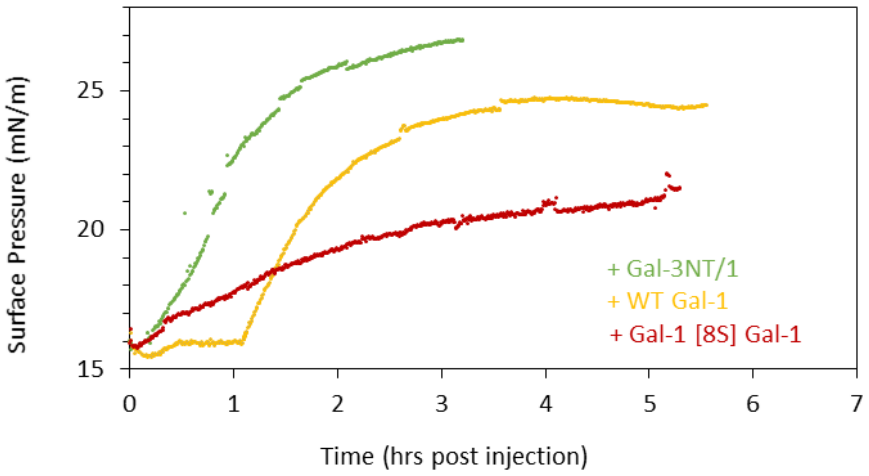

Figure 2. Surface pressure constantly rises after insertion of each protein into the 89.5:5:0.5 DPPC:GM1:TexasRed-DHPE membrane.

These observations may be due to the clustering and oligomerization of the proteins inserted. Gal-3/NT1 has a collagen like repeat tail that is known to induce clustering in WT Gal-3. Gal-1 [8S] Gal-1 had the most notable effects on the decrease of the lipid condensed domain, likely due to the mutant linker between the two carbohydrate binding domains. The coherence lengths also increased upon protein interaction; the monolayer without protein exhibited an L_c of 59Å while the proteins produced an L_c of ~67 Å.

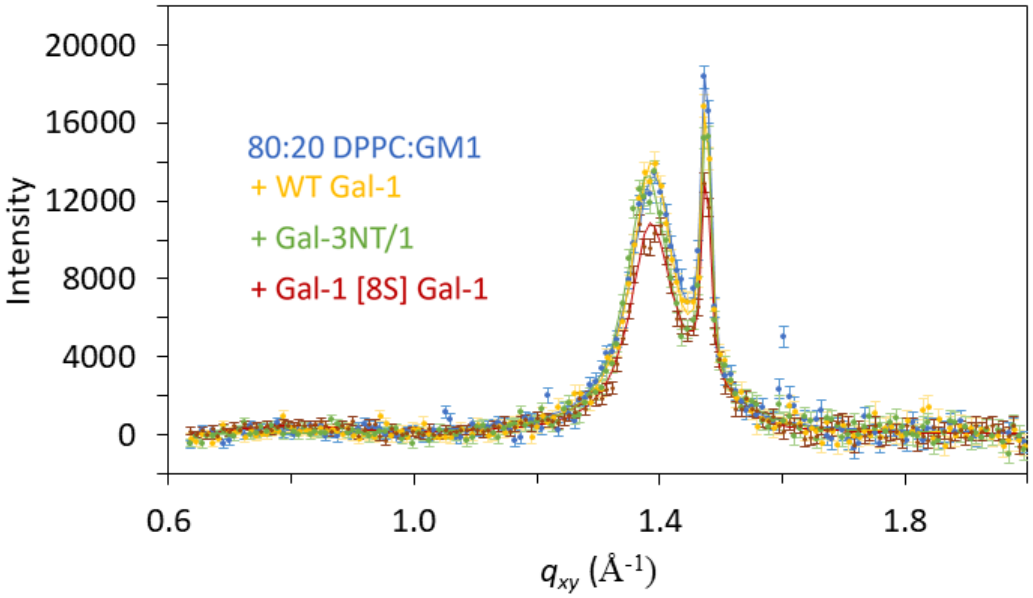

Figure 3. Diffraction peaks obtained from GIXD scans of the membrane and protein variants.

Sample	q_{xy} Position (Å^{-1})	FWHM	d Spacing (Å)	Integrated Peak Area	Coherence Length L_c (Å)
		Protein + DPPC:GM1: Lipid Diffraction Peaks			
80:20 DPPC:GM1	1.400 ± 0.007	0.095 ± 0.003	4.52 ± 0.02	1970 ± 60	59 ± 2
	1.476 ± 0.006	0.0163 ± 0.0012	4.258 ± 0.018	470 ± 20	370 ± 30
+ WT Gal-1	1.387 ± 0.007	0.084 ± 0.003	4.53 ± 0.02	1840 ± 50	66 ± 2
	1.475 ± 0.006	0.0184 ± 0.0013	4.259 ± 0.018	450 ± 20	320 ± 0
+ Gal-3NT/1	1.380 ± 0.007	0.084 ± 0.004	4.55 ± 0.02	1700 ± 100	67 ± 3
	1.476 ± 0.006	0.0134 ± 0.0019	4.256 ± 0.018	360 ± 30	470 ± 70
+ Gal-1 [8S] Gal-1	1.385 ± 0.008	0.077 ± 0.003	4.54 ± 0.03	1400 ± 100	67± 2
	1.476 ± 0.006	0.0185 ± 0.0015	4.257 ± 0.018	270 ± 30	470 ± 80

Table 1. Data collected on peaks obtained from the fit of the GIXD data

XR

XR data was collected at 2 hours and 5 hours post injection. The earlier scans did not contain enough contrasting data to be included in analysis so only the 5-hour time points are used (Fig. 4). The SLD plots show the regions of electron density “slabs” associated with the lipid tails, head, glycans, and proteins. In order to determine the significance of the protein layer in the scans, the membrane and WT Gal-1 scans were both fit in Igor Pro using three slab and four slab models (Fig. 5). This comparison allowed for the determination of the significance of the fourth layer in following reflectivity fits.

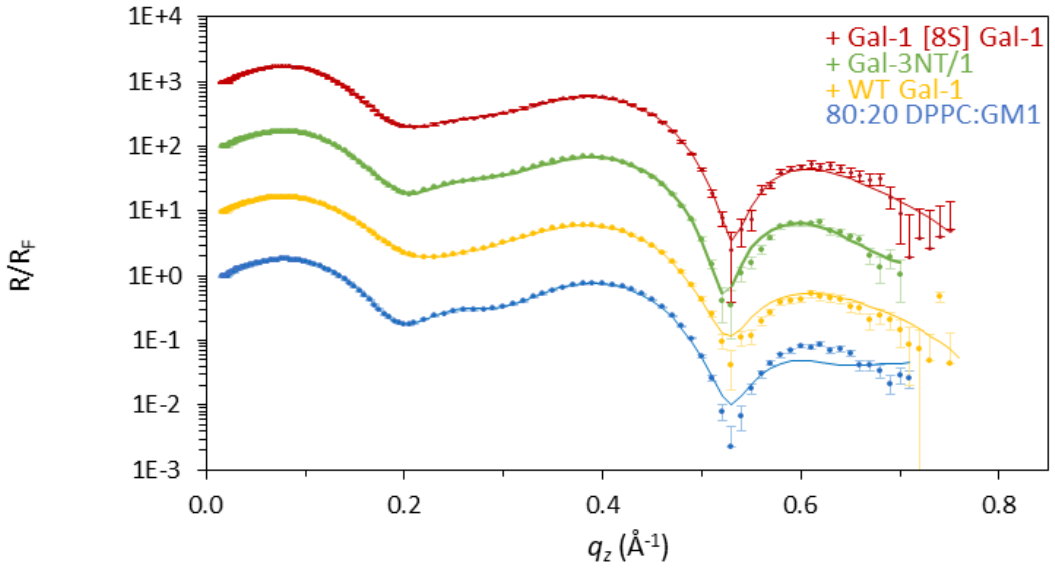

Figure 4. Reflectivity scans of the membrane and membrane with proteins inserted 5 hours post injection. The reflectivity data is offset for graphing.

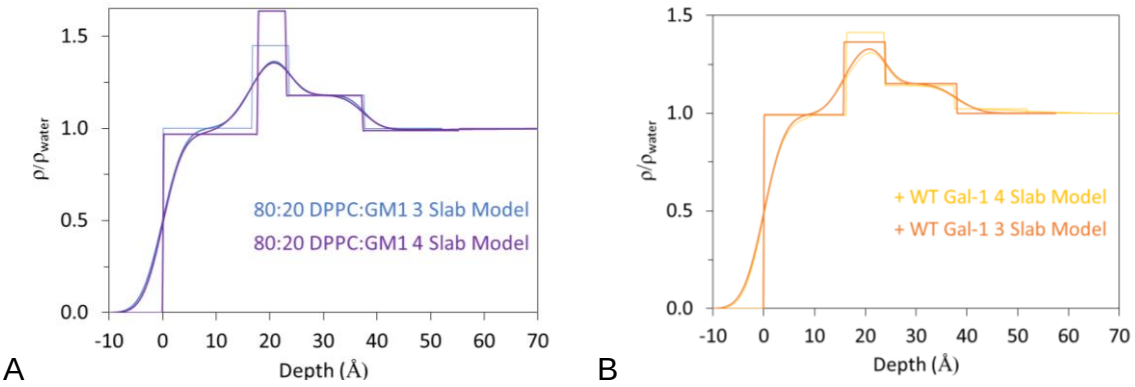

Figure 5. (A) Comparing the three-slab model against the four-slab model for the 80:20 DPPC:GM1 membrane. The fourth slab did not exceed the electron density of water and barred no statistical significance. (B) Comparing the three-slab model against the four-slab model of WT Gal-1. The four-slab model exhibited statistical significance as the electron density of the fourth slab was higher than that of water.

The four-slab model of the membrane scan did not produce a fourth electron density (0.990+/-0.010 ρ/ρ_w) significantly larger than water (1.0 ρ/ρ_w). This fit also had extremely high error margins and a high χ^2 value (8.5), indicating the three-slab model was the best fit out of the two. The three-slab model of WT Gal-1 had similar discrepancies with a higher χ^2 value (7.2) than that of the four-slab model as seen in Table 2. The electron density of the four-slab model allowed for the electron density of each protein to be measured separate from the glycan groups, each of which had a statistically significant difference from water (Table 2). Confirming the validity of the protein layer in the SLD plot allows us to compare the SLD profiles of each scan (Fig. 6).

	Slab 1 (Tails)			Slab 2 (Heads)			Slab 3 (Glycans)			Slab 4 (Protein)			Subphase	
Sample	Thickness	ρ / ρ_{water}	Roughness	Thickness	ρ / ρ_{water}	Roughness	Thickness	ρ / ρ_{water}	Roughness	Thickness	ρ / ρ_{water}	Roughness	Roughness	χ^2
80:20 DPPC:GM1	16.6 ± 0.3	1.002 ± 0.007	3.18 ± 0.06	6.8 ± 0.4	1.452 ± 0.017	3.4*	14.15 ± 0.12	1.183 ± 0.002	2.4*	/	/	/	2.37 ± 0.12	6.9
+ WT Gal-1	16.3 ± 0.4	0.9587 ± 0.0014	3.04*	7.5 ± 0.5	1.41 ± 0.03	4.6 ± 0.2	13.66 ± 0.16	1.1416 ± 0.0015	2.35 ± 0.14	14.5 ± 1.6	1.022 ± 0.003	2.9*	8.3 ± 1.6	2.17
+ Gal-3NT/1	16.3 ± 0.3	0.9762 ± 0.0013	3.07*	7.7 ± 0.5	1.39 ± 0.02	3.75 ± 0.19	13.3 ± 0.2	1.171 ± 0.002	2.03 ± 0.15	12.2 ± 1.9	1.034 ± 0.005	2.05*	9.4 ± 1.7	1.8
+ Gal-1 [8S] Gal-1	16.1 ± 0.6	0.9800 ± 0.0018	3.21*	7.7 ± 1.0	1.39 ± 0.05	3.9 ± 0.24	13.1 ± 0.3	1.184 ± 0.003	2.0 ± 0.4	9 ± 3	1.038 ± 0.017	2.7 ± 0.3	5.2 ± 1.8	1.5

*This value was fixed to reduce the number of parameters in fitting.

Table 2. Values deduced from the scattering length density (SLD) of the membrane and three protein variants. The electron density of the fourth protein layer is statistically significant for each protein sample.

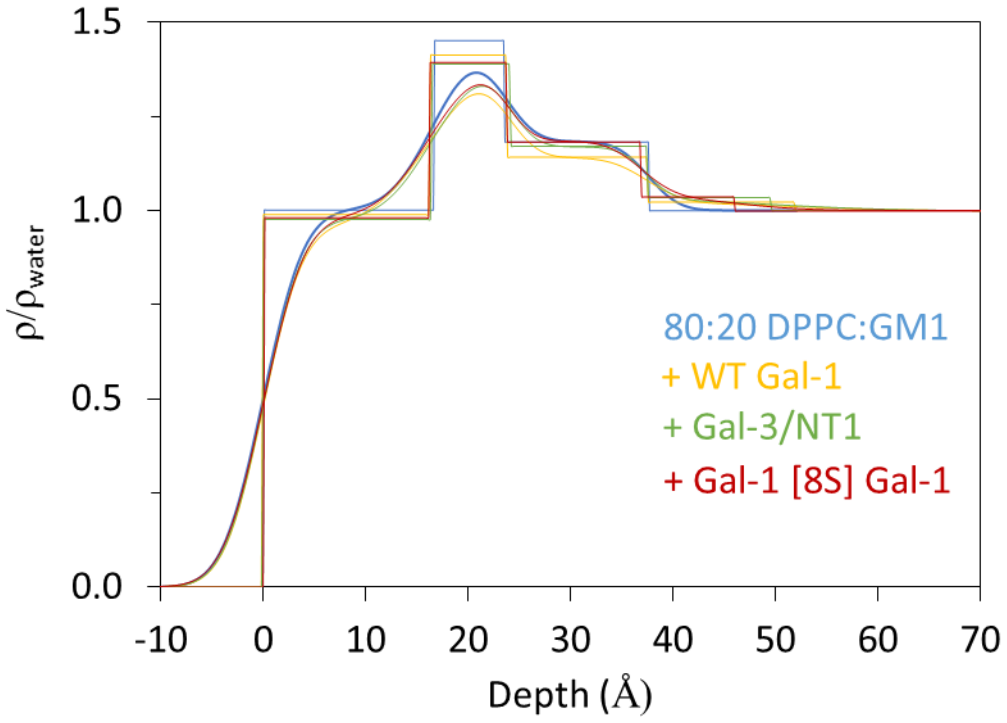

Figure 6. SLD profiles of the membrane and 3 protein variants. The fourth layer of each protein fit depicts the electron density and length of the protein or portion of protein protruding from the membrane. The curved lines are the raw data collected and the straight lines are the slab model fits. The y-axis is the electron

density of the slabs relative to water and the x-axis is the thickness of the slab layers.

Discussion

Langmuir trough and x-ray scattering data of DPPC/GM1 monolayer at their air/water interface before and after injection of WT Gal-1 and mutants have been presented. We studied the 95:5 mol% DPPC:GM1 (trough only) and the 80:20 mol% DPPC:GM1 monolayer (x-ray scattering only) before injection protein variants underneath the stable monolayer using a Hamilton syringe. A final protein concentration of 0.0125 mg/mL was used in both the Langmuir trough and x-ray scattering experiments. Surface pressure increases in the Langmuir trough experiments indicate that the proteins studied do in fact interact with the monolayer. Gal-3NT/1 induced the highest surface pressure increase and also exhibited the fastest insertion rate compared to Gal-1 [8S] Gal-1. Gal-1 [8S] Gal-1 increased the surface pressure the least over the measured time and had the slowest rate of insertion, consistent with less insertion into the membrane. WTGal-1 had a lag of about 1 hour before it began increasing surface pressure due to experimental error (the barriers were not fixed which resulted in area expansion, not surface pressure increase).

In contrast to the slow insertion and lower increase of surface pressure by Gal-1 [8S] Gal-1, this protein had the most dramatic GIXD results. It lowered the integrated molecular area and peak intensity more than the other proteins studied, indicating that this mutant had the most membrane disrupting capability. Gal-3NT/1 had the second largest effect on the condensed lipid domains seen by

the decrease in area and intensity of the peaks. This effect is likely due to the ability of the collagen like tails of this mutant to aggregate and form disordered clusters. WT Gal-1 had the smallest effects on the packing of the membrane compared to the other protein mutants. This protein however did still disrupt the lipid ordered domains and induced a similar increase in coherence length as the other proteins did. Each of these proteins likely is able to oligomerize and cluster upon interaction with lipid condensed domains and acquire different positions within the membrane, thus disrupting the packing structure but not the organization of the lipid condensed domains. It is evident that these interactions do take placed in lipid condensed phases; if they had not, the GIXD scans would be identical for each sample.

In supplement to the GIXD data, XR was used to elucidate the electron density distribution along the vertical plane of the monolayer. Scanning of the monolayer prior to protein injection show the lipid tails and headgroups in two distinct slabs within a slab model, with the glycans protruding from the headgroups constituting a third slab of electron density. The electron density distributions of samples after protein injection show weak evidence of proteins interacting with the glycan group of GM1. The presence of a fourth slab of electron density is present within these scans, corresponding to the given protein interaction. The decrease of electron density in the headgroups within these scans is likely due to slight protein insertion into the headgroups. Due to the lack of electron density increase in the other slabs, it is unlikely the CRDs are making

contact with the hydrophobic lipid tails. The SLD profile only suggests peripheral interactions with the glycan groups.

Conclusion

Based on the experiments conducted, there is clear evidence of galectin-1 and its variants interacting with the model membrane by means of ganglioside GM1. These interactions are found throughout the body and induce propagated cell signaling pathways, especially in neuronal cells. The evidence collected suggests that the proteins interact with the membrane and reduce the presence of liquid condensed domains due to the dynamic oligomerization or clustering of proteins. Within the GIXD experiments, the mutants exhibited greater condensed domain disruption likely because of their long linker/tail domains' ability to interact at a greater capacity than WT Gal-1 which lacks these long repeats. Future studies should be done with greater protein concentration and for longer periods of time to create a more robust and all-encompassing profile of these interactions. The addition of cholesterol into the membrane *could* provide another insight into how these interactions may behave in vivo as it has been noted that the steroid reduces GM1 and Gal-1 contact. There may be a mutant that can bypass the effects of cholesterol inhibition which would provide insight on how these molecules can eventually be optimized for therapeutic use. Experiments such as this, and others examining different membrane interactions will contribute to the decoding of the glycocode, and potentially allow for future therapeutic advancement. It is important to keep studying these extremely complex and variable interactions in order to map the effects of cell signaling by

the sugar code, so that therapeutic use of these pathways is possible without triggering undesired effects.

References

(1) Arnaud, J.; Tröndle, K.; Claudinon, J.; Audfray, A.; Varrot, A.; Römer, W.; Imberty, A. Membrane Deformation by Neolectins with Engineered Glycolipid Binding Sites. *Angew. Chemie - Int. Ed.* 2014. https://doi.org/10.1002/anie.201404568.

(2) Rapoport, E. M.; Kurmyshkina, O. V.; Bovin, N. V. Mammalian Galectins: Structure, Carbohydrate Specificity, and Functions. *Biochemistry (Moscow)*. 2008. https://doi.org/10.1134/S0006297908040032.

(3) Gabius, H. J. Probing the Cons and Pros of Lectin-Induced Immunomodulation: Case Studies for the Mistletoe Lectin and Galectin-1. *Biochimie*. 2001. https://doi.org/10.1016/S0300-9084(01)01311-6.

(4) Murphy, P. V.; André, S.; Gabius, H. J. The Third Dimension of Reading the Sugar Code by Lectins: Design of Glycoclusters with Cyclic Scaffolds as Tools with the Aim to Define Correlations between Spatial Presentation and Activity. *Molecules*. 2013. https://doi.org/10.3390/molecules18044026.

(5) Arcolia, V.; Journe, F.; Wattier, A.; Leteurtre, E.; Renaud, F.; Gabius, H. J.; Remmelink, M.; Decaestecker, C.; Rodriguez, A.; Boutry, S.; Laurent, S.; Saussez, S. Galectin-1 Is a Diagnostic Marker Involved in Thyroid Cancer Progression. *Int. J. Oncol.* 2017. https://doi.org/10.3892/ijo.2017.4065.

(6) Chernyy, E. S.; Rapoport, E. M.; Andre, S.; Kaltner, H.; Gabius, H. J.; Bovin, N. V. Galectins Promote the Interaction of Influenza Virus with Its Target Cell. *Biochem.* 2011. https://doi.org/10.1134/S0006297911080128.

(7) Nelson, D. L.; Cox, M. M. *Lehninger Principles of Biochemistry, Seventh Edition*; 2013. https://doi.org/10.1016/j.jse.2011.03.016.

(8) Ledeen, R. W.; Wu, G. The Multi-Tasked Life of GM1 Ganglioside, a True Factotum of Nature. *Trends in Biochemical Sciences*. 2015. https://doi.org/10.1016/j.tibs.2015.04.005.

(9) Wang, J.; Lu, Z.-H.; Gabius, H.-J.; Rohowsky-Kochan, C.; Ledeen, R. W.; Wu, G. Cross-Linking of GM1 Ganglioside by Galectin-1 Mediates Regulatory T Cell Activity Involving TRPC5 Channel Activation: Possible Role in Suppressing Experimental Autoimmune Encephalomyelitis. *J. Immunol.* 2009. https://doi.org/10.4049/jimmunol.0802981.

(10) Als-Nielsen, J.; Jacquemain, D.; Kjaer, K.; Leveiller, F.; Lahav, M.; Leiserowitz, L. Principles and Applications of Grazing Incidence X-Ray and Neutron Scattering from Ordered Molecular Monolayers at the Air-Water Interface. *Physics Reports*. 1994. https://doi.org/10.1016/0370-1573(94)90046-9.

(11) Als-Nielsen, J.; Kjær, K. X-Ray Reflectivity and Diffraction Studies of Liquid Surfaces and Surfactant Monolayers; 1989. https://doi.org/10.1007/978-1-4613-0551-4_11.

(12) Jensen, T. R.; Kjaer, K. Structural Properties and Interactions of Thin Films at the Air-Liquid Interface Explored by Synchrotron X-Ray Scattering. In *Studies in Interface Science*; 2001. https://doi.org/10.1016/S1383-7303(01)80028-4.